Preparation of Nanostructured Pd-C-Ru Composite Electrodes for Alcohol Electrooxidations. Part-I: A Study of Ethanol Oxidation by Cyclic Voltammetry and Impedance Spectroscopy

Anindita, R. Awasthi, Madhu and R.N. Singh*

Department of Chemistry, Faculty of Science, Banaras Hindu University, Varanasi-221005, India

Abstract: Ternary nanocomposite films of Pd, Ru and nanocarbon (C) are obtained on glassy carbon (GC) and studied by XRD, TEM, cyclic voltammetry (CV), impedance and chronoamperometric techniques for their use as electrocatalysts for ethanol oxidation reaction (EOR). Results show that introduction of Ru to the Pd-0.5wt%C composite electrode increases the electrocatalytic activity greatly. It is observed that with Ru addition from 1 to 50 wt%, the rate for EOR initially increases, attains a maximum (at 20wt %) and declines thereafter. Further, among the electrocatalysts investigated, the Pd-0.5wt%C-20wt% Ru electrode has displayed the greatest electrocatalytic activity. This electrode has nearly two times higher activity than the base electrode (Pd-0.5wt%C).

Keywords: Alcohol oxidation; Electrocatalytic properties; Nanocomposites; Direct ethanol fuel cells (DEFCs).

1. INTRODUCTION

The direct alcohol fuel cells (DAFCs) appear to be the most promising as a power source for portable applications such as cellular phones and laptop computers and also for transportation applications such as automobiles and buses [1]. Small alcohol molecules, such as methanol, ethanol, ethylene glycol and glycerol, exhibit high volumetric energy densities and their storage and transport are much easier as compared to hydrogen [2, 3]. The most common DAFC is the direct methanol fuel cell (DMFC). But, owing to toxicity of methanol, the direct ethanol fuel cell (DEFC) is receiving increasing interests during recent years [4]. Pt-based metals and alloys such as PtRu are known as the best catalysts for oxidation of alcohols in acid solutions [5]. However, they undergo poisoning by the oxidation intermediates, particularly CO molecule [6-9]. Also, they are pretty costly and have poor abundance on earth. It is, therefore, of interest to search out new catalytic materials for DAFC anodes that do not contain Pt or contain tiny amounts of this rare metal and are capable to effectively oxidize alcohols.

In recent years, Pd is considered as the most suitable replacement for Pt in DAFCs. It is because of the fact that, unlike Pt based electrocatalysts, they can be highly active for the oxidation of a large variety of substrates in alkaline environment where non-noble metals are also sufficiently stable for electrochemical applications. Pd with non-noble metals in a smart catalytic architecture can be capable of rapidly and stably oxidizing alcohols on anode electrodes. Also, Pd is more abundant in nature and less expensive than Pt [10].

*Address correspondence to this author at the Department of Chemistry, Faculty of Science, Banaras Hindu University, Varanasi-221005, India; Tel: +91-542-6701596; Fax: +91-542-2368127; E-mail: rnsbhu@rediffmail.com

Considerable research work has recently been carried out [11-16] to improve the catalytic efficiency of Pd-catalysts by suitable means. Bambagionia *et al.* [17] obtained Pd nanoparticles on MWCNTs (multiwalled nanocarbon tubes) by the impregnation-reduction procedure. The Pd/MWCNT electrode exhibited the high activity for the oxidation reaction of methanol, ethanol and glycerol in 2 M KOH, even at metal loadings as low as 17-20 μg cm^{-2}. However, this electrode is electrochemically stable only for the oxidation of ethanol. The degradation of the electrode during methanol and glycerol oxidations has been ascribed [3, 17-19] to the formation of adsorbed CO. Ethanol is selectively oxidized to acetic acid which soon gets transformed into acetate ion.

Shen *et al*. [20] demonstrated that the electroless reduction of $PdCl_2$ adsorbed onto oxide/C materials (oxides: CeO_2, Co_3O_4, Mn_3O_4, NiO) yields electrocatalysts for alcohol oxidation with much higher catalytic activity and electrochemical stability.

Hu *et al.* [21] Prepared Pd nanoparticles on tungsten carbides modified MWCNTs by an intermittent microwave heating (IMH) technique. The Pd-WC/MWCNT catalysts showed highly improved kinetics for ethanol oxidation in 1 M KOH + 1 M C_2H_5OH. Following IMH technique Hu *et al*. [22] also prepared NiO supported Pd/C electrocatalysts. The electrocatalyst with ratio of Pd to NiO equal to 1:1 gave the best performance for ethanol oxidation in alkaline solution.

Chu *et al.* [23] obtained Pd-In_2O_3/CNTs composite catalysts by using chemical reduction and hydrothermal reaction process. It was observed that addition of In_2O_3 nanoparticles into Pd significantly promotes the catalytic activity for ethanol electrooxidation in comparison to the Pd/CNT (carbon nanotube) electrode.

Wang *et al.* [13] and Zhang and Li [14] obtained composites of Pd, TiO_2 nanotubes and C and demonstrated

1876-214X/11 2011 Bentham Open

that the composite films were much superior to that of pure Pd in respect of electrocatalysis of the methanol oxidation reaction (MOR) in acid medium. Zhang *et al.* [15] obtained well dispersed Pd nanoparticles on the surface of vanadium oxide nanotubes (VO_x-NTs) through a simple reductive process. The new materials were found to exhibit excellent electrocatalytic activities and good stability under alkaline condition. Shen and Xu [16] observed that the presence of NiO into the Pd/C composite improves the electrocatalytic activity of the electrode considerably. The electrode with a weight ratio of Pd to NiO of 4:1 exhibited the highest electrocatalytic activity for methanol oxidation in alkaline medium. Bianchini *et al.* [24] studied the ethanol oxidation reaction (EOR) on Pd-(Ni-Zn)/C and Pd/C (C = Vulcan XC-72) in 2 M KOH. They demonstrated that the oxidation of ethanol to acetic acid can be selectively achieved on Pd-based catalysts. Bagchi and Bhattacharya [25] investigated the EOR on Pd-Ru alloy in 1 M KOH and demonstrated that the electrode containing the higher amount of deposit are less affected by carbonaceous poison. Fang *et al.* [26], in a spectroelectrochemical study of electrooxidation of ethanol on Pd electrode, observed that the electrode performance depends on the pH of the fuel solution. They found the best performance in 1 N NaOH (pH = 14) while the electrochemical activity decreased by either increasing or decreasing NaOH concentration. The FTIR spectroscopic measurements showed sodium acetate as the main oxidation product at NaOH concentration > 0.5 M. The C-C bond cleavage of ethanol occurred at pH 13.

Singh *et al*. [27-29] obtained nanocomposite films of Pd and MWCNTs and of Pd and nanocarbon (C) for use as electrocatalysts for the EOR [27-28] and MOR [29, 30] in alkaline solutions. Results have demonstrated that a low content of MWCNTs/C in the composite improves the electrocatalytic activity of the electrode greatly. In contrast, its higher contents (> 1wt% MWCNT or 0.5wt% C) decreased the activity. The electrocatalytic activity of the composite electrode was the greatest with 1wt% MWCNTs ($I_p \approx 465$ mA mg_{Pd}^{-1}, $E_P \approx 0.125$ V *vs* Hg/HgO in 1M KOH + 1M C_2H_5OH) and 0.5wt% C ($I_p \approx 438$ mA mg_{Pd}^{-1}, $E_P \approx -0.08$ V *vs* Hg/HgO in 1M KOH + 1M C_2H_5OH). They also observed [31] that addition of Ni from 1 to 20% to the pure Pd electrode increased the electrocatalytic activity for alcohol (ethanol, methanol, ethylene glycol, glycerol) electrooxidation showing maximum with 10% Ni ($I_p \approx 377$ mA mg_{Pd}^{-1} $E_p \approx -0.01$ V *vs* Hg/HgO in 1M KOH + 1M C_2H_5OH). Incorporation of C from 0.5 to 10% to the active Pd-10% Ni composite improved the electrocatalytic performance of the electrode further ($I_p \approx 783$ mA mg_{Pd}^{-1}, $E_P \approx 0$ V *vs* Hg/HgO in 1M KOH + 1M C_2H_5OH). Bambagioni *et al.* [17] also prepared Pd-supported on MWCNTs and investigated as electrocatalysts for oxidation of methanol, ethanol and glycerol in deoxygenated 2 M KOH solution. The electrocatalysts exhibited high activities for oxidation of each alcohol ($I_p \approx 2100$ mA mg_{Pd}^{-1}, $E_p \approx -0.12$ V *vs* $Ag/AgCl/KCl_{sat}$ in 2M KOH + 10% C_2H_5OH) even at metal loadings as low as 17-20 mg cm^{-2}. The rate of oxidation followed the order glycerol > ethanol > methanol. To improve the electrocatalytic activity further, Ru was added from 1 to 50 wt% to the Pd-0.5wt% C composite and investigated the structural and electrocatalytic properties of the new products, so derived, in relation to MOR and EOR in 1 M KOH. Similar study seems to have not been reported in literature. However, the influence of Ru addition on the electrocatalytic properties of Pt towards alcohol oxidation in acid solutions has been studied [3, 32-34] considerably. This paper describes the results of the present investigation.

2. EXPERIMENTAL

2.1. Electrocatalyst Preparation

Binary composites of Pd and 0.5wt% C and Ru and 0.5wt% C and ternary composites of Pd, 0.5wt% C and Ru were prepared by sodium borohydride reduction method as previously described [27]. Ternary composites prepared were those containing 1, 2, 5, 10, 20, 30, and 50wt%Ru. To obtain a ternary composite of Pd, Ru and C, the required amounts of $PdCl_2$ and $RuCl_3$ were dissolved in 5 ml acidified double distilled water, added the required amount of nanocarbon (C) powders and then ultrasonicated for 15 min. After 1 h, an excess amount of $NaBH_4$ solution was added in drop-wise manner under stirred condition so as to carry out the complete reduction of the metal ions. The catalyst formed as solid residue in the solution, was centrifuged, repeatedly washed with double distilled water and finally dried overnight in a vacuum oven at 373 K. The composition of constituents of composite materials given in the text is based on their respective amounts taken for preparation.

Prior to use in the preparation of the composites, nanocarbon powders (Aldrich, 99+ %, particle size ≤ 30 nm, BET surface area > 100 $m^2 g^{-1}$) were activated by refluxing in concentrated HNO_3 for 5 h as described elsewhere [35]. Other chemicals, namely $PdCl_2$ (anhydrous: Merck, Pr. No. 61777900011730), $RuCl_3$ hydrate (Aldrich, 99.98%, Pr. No. 463779) and $NaBH_4$ (Sigma-Aldrich, Pr. No. 452874) were used as received.

2.2. Electrode Preparation

The catalyst obtained in powder form was mixed with few ml of ethanol-water (2:1) mixture and then ultrasonicated for 15 min to obtain an ink. 2-3 drops of ink were placed on to a pretreated Glassy carbon (GC) plate through a syringe, dried and then one drop of 1% Nafion solution (Alfa Aesar) was dropped over the dried catalyst layer to cover it. The catalyst loaded GC plate was then irradiated with microwave (800 watt) for 1 min. Prior to use as support for the catalyst, GC plates were first polished well on a polishing machine, using a micro cloth pad and alumina powders and then dipped in 0.2 M H_3PO_4 for 5 min, degreased in acetone by ultrasonication, washed with distilled water and dried. Electrical contact with the catalyst overlayer and electrode mounting were obtained as given in [36, 37]. The loadings of the catalytic film on GC and Nafion on the catalyst over layer were 0.15 - 0.23 and ~0.10 mg cm^{-2}, respectively.

2.3. Material Characterization

X-ray diffraction (XRD) patterns of composite films on GC were recorded on an X-ray diffractometer (Thermo Electron) using CuKα as the radiation source (λ = 1.541841 Å). Morphology of the catalytic films has been studied by a

transmission electron microscope (TECNAI G^2 FEI). To obtain TEM pictures, the catalyst was dispersed in methanol and a drop of this suspension was placed onto a carbon coated copper grid, and dried.

2.4. Electrochemical Studies

A conventional three-electrode single compartment Pyrex glass cell was used to carry out electrochemical studies. The reference and counter electrodes were Hg/HgO/1 M KOH and Pt foil (~8 cm^2), respectively. Cyclic voltammetry (CV), impedance and chronoamperometry studies were performed using an EG&G PAR model 273A galvanostat/potentiostat. The CV experiments were carried out in the potential range from 0.126 to 1.526 V *vs* RHE. In each experiment, the composite electrode in the electrolyte was first cycled for 5 runs at the scan rate of 50 mV s^{-1} in the said potential region so as to obtain a reproducible voltammogram. The impedance study of the electrocatalysts has been carried out in alkaline ethanol solutions with the ac voltage amplitude of 10 mV at a constant dc potential. The frequency range employed in the study was 0.01 - 10 x 10^3 Hz. The equivalent circuit parameters were analyzed by using the software, ZsimpWin. All electrochemical experiments were performed in an Ar deoxygenated electrolyte at 298 K. The potentials of the working electrode were measured using the reference, Hg/HgO/1M KOH (E° = 0.098 V *vs* SHE), but values given in the text are against the reversible hydrogen electrode, RHE (E° = - 0.828 V *vs* SHE).

It is mentioned that electrochemical data have been obtained with triplicate electrodes of each type of composites and the results reported in the text are average ones; only the impedance study was carried out using a single electrode of the catalyst.

3. RESULTS AND DISCUSSION

3.1. XRD/TEM

Fig. (**1**) shows the XRD patterns of nanostructured Ru-0.5wt% C, Pd-0.5wt% C, Pd-0.5wt% C-1wt% Ru, Pd-0.5wt% C-10 wt% Ru, Pd-0.5wt% C-20wt% Ru and Pd-0.5wt% C-50wt% Ru composite films on glass. To avoid the contribution of glassy carbon (GC) support in diffractograms, composite films were obtained on glass. Features of all the difractograms displayed in Fig. (**1**) indicate that the composite materials are in either amorphous phase or have very small particle sizes. Further, with the exception of Ru-0.5wt% C and Pd-0.5wt% C-50wt% Ru all the composite films indicate the presence of the three characteristic peaks for the face centered cubic (fcc) structure of Pd in their diffractograms shown in (Fig. **1**). These peaks are found at 2θ ≈ 40º (d = 2.253 Å), ≈ 46.6º (d = 1.95 Å) and ≈ 68º (d = 1.371 Å) and can be assigned to (111), (200) and (220) planes, respectively. An addition of Ru (1 - 10 wt%) does not indicate the formation of any significant new phase, however, it slightly increases the d-value for the 100% peak of pure Pd, the magnitudes of increment being ranged from 0.006 - 0.011 Å. Thus, the

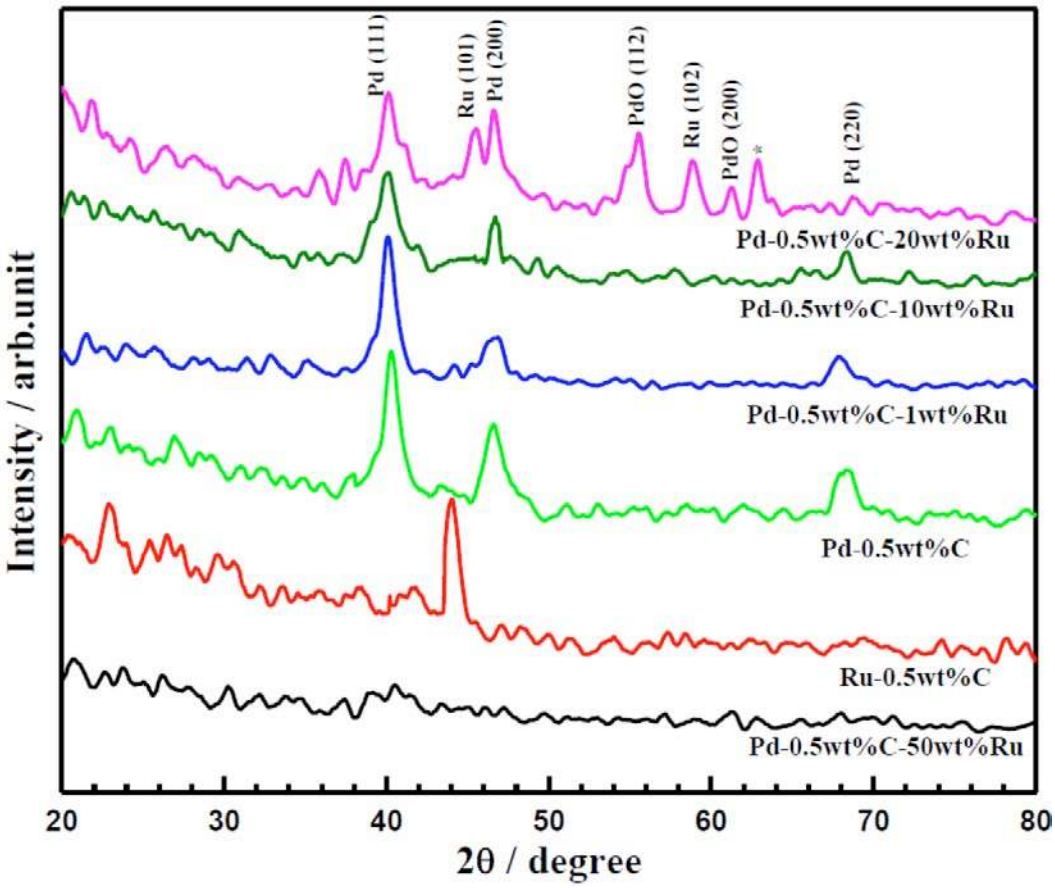

Fig. (1). XRD patterns of Pd-0.5wt% C, Ru-0.5wt%C, Pd-0.5wt%C-1wt%Ru, Pd-0.5wt%C-10wt%Ru, Pd-0.5wt%C-20wt%Ru and Pd-0.5wt%C-50wt% Ru as deposited on glass electrode.

result indicates the formation of a solid solution of Ru in Pd [31,38]. However, the diffractogram for the composite with 20wt% Ru exhibits a few additional diffraction peaks at 2θ = 45.02º (d = 2.0135 Å) and 58.73º (d = 1.572 Å) and 2θ = 55.48º (d = 1.656 Å) and 61.18º (d = 1.515 Å), which can be assigned to the formation of Ru (JCPDS 06-0663) and PdO (JCPDS 43-1024) phases in the composite, respectively. Further, the diffraction peak corresponding to 2θ = 62.78º (d = 1.48 Å) remains unidentified. On the other hand, the composite containing 50wt% Ru showed an amorphous phase.

The Pd (111) diffraction peak was used to calculate the crystallite size of Pd in different catalysts according to Scherrer equation. Estimates of the average crystallite size of Pd in Pd-0.5wt%C, Pd-0.5wt% C-1wt% Ru, Pd-0.5wt% C-5wt% Ru, Pd-0.5wt% C-10wt% Ru, and Pd-0.5wt% C-20wt% Ru catalysts are ~8, ~9, ~7, ~6, and ~11 nm, respectively.

TEM pictures of pure Pd and some composite electrodes, namely, Pd-0.5wt% C, Pd-0.5wt% C-5wt% Ru and Pd-0.5wt% C-20wt% Ru are shown in Fig. (**2a-h**). From Fig. (**2**) it seems that Pd and Pd-Ru nano-particles are deposited at the surface of the carbon particles. The deposited particles look like nanopeanuts and organize to produce a network of clusters. The average particle sizes are found to be ~12, ~10, ~5, and ~4 nm respectively in pure Pd, Pd-0.5wt% C, Pd-0.5wt% C-5wt% Ru and Pd-0.5wt% C-20wt% Ru nanocomposites. Thus, both 0.5wt% C and 5wt% Ru-additions decrease the particle size, the effect, however, being significant in the case of the latter. The higher addition of Ru (20wt%) does not influence the size significantly.

On selected area the electron diffraction patterns of the catalysts (Fig. **2b**, **d**, **f**, **h**) show that the composite materials are crystalline. The d-values and hence, the corresponding planes of Pd were estimated based on the radius of concentric rings obtained in case of different composites. Estimates of *d*-values were ~2.206, ~1.93, ~1.345, ~1.135 and ~0.85 Å and the corresponding planes were (111), (200), (220), (222) and (420). Thus, the results are in good agreement with the literature values of *d* for pure Pd (JCPDS 05-0681).

3.2. Cyclic Voltammetry (CV)

Figs. (**3**, **4**) show CVs of Pd-0.5wt% C-x wt% Ru (x = 1, 2, 5, 10, 20, 30 and 50) at a scan rate of 50 mV s^{-1} in 1 M KOH with and without containing 1 M C_2H_5OH at 298 K. CVs of the composite electrodes in 1M KOH were quite similar and a representative voltammogram for Pd-0.5wt% C-20wt% Ru is shown in Fig. (**3**). This voltammogram exhibits a strong cathodic peak (at E = 0.536 V *vs* RHE) for the reduction of palladium oxide which is formed as a result of the Pd surface oxidation at E > 0.536 V *vs* RHE under anodic condition. The potential region between 0.126 and 0.426 V *vs* RHE corresponds to the adsorption-desorption of hydrogen. Similar voltammograms were also found on Pd-x wt% MWCNT (x = 1, 2, 5) in 1 M KOH [26]. To examine the influence of introduction of Ru on the electrochemical feature of the composite electrode, two more CV curves, one for Pd-0.5wt% C and the other one for Ru-0.5wt% C, are also given in Fig. (**3**). These curves show that Ru addition does not change the feature of CV curve for the base (Pd-0.5wt% C) electrode practically.

Fig. (**4**) gathers CV curves of the composite electrodes in 1 M KOH + 1 M C_2H_5OH at 298 K. The comparison of CVs of the composite electrodes recorded in the blank solution (1 M KOH) with those obtained in 1 M KOH + 1 M C_2H_5OH clearly demonstrates significant oxidation of C_2H_5OH as indicated by two well defined anodic peaks, one observed on the forward and other one, observed on the reverse scan. Two similar anodic peaks were also found on Pd electrodeposited on Ti in 1 M KOH + 1 M C_2H_5OH [36]. As already reported [33, 39], the observed oxidation peak during the forward scan is due to the oxidation of adsorbed ethanol molecules. At higher potential value the electrode is passivated due to the formation of a Palladium-ruthenium oxide layer. On the negative-going scan the anodic currents are due to ethanol oxidation as well, reflecting the ethanol oxidation on the catalyst surface free from oxides, which were formed previously at higher potentials. Further, the observed hydrogen adsorption-desorption region (i.e. from 0.126 to 0.426 V *vs* RHE) (Fig. **3**) appears to be completely suppressed when ethanol is present in solution (Fig. **4**). This is because of the fact that the onset potentials (E_{op}) for the EOR ($E_{op} \approx 0.286 - 0.376$ V *vs* RHE) on composite electrodes (Table **1**), exactly fall in the potential region wherein the hydrogen adsorption-desorption reactions take place. The latter reactions are dominated by the ethanol oxidation reaction. The E_{op} was determined by extending the initial linear part of the anodic curve for the forward scan towards the higher potential side and noting the potential corresponding to the point on the linear curve from where the anodic curve begins to rise. In the forward scan, the observed decrease in the oxidation current peak, I_P (i.e. self inhibition of alcohol oxidation) can be ascribed to the surface poisoning induced by irreversible strong adsorption of some CO-like species [1, 32, 40]. The latter gets deposited on the active site of Pd and thereby inhibits the adsorption of alcohol molecule and hence the rate of its oxidation. At higher potentials, adsorbed CO species can be effectively removed by reaction with OH_{ad} that is produced in the oxygen–adsorption region. CV curves of Fig. (**4**) were analyzed for the onset potential (E_{op}), the peak current (I_p), and the peak current potential (E_p) and values, so obtained, are listed in Table **1**.

Table **1** and Fig. (**4**) show that introduction of Ru from 1 to 20wt% shifts the E_{op} for the EOR towards less noble side; a reversal in direction of the shift is observed when x > 20wt%. However, the overall shift in E_{op} is negative with each Ru substitution compared to one observed in the case of Pd-0.5wt% C. Thus, Ru addition to Pd-0.5wt% C seems to be beneficial from electrocatalysis view point, which is quite evident from the observed marked increase in the peak current value with progressive addition of Ru from 1 to 20wt%. A decline in the peak current, however, takes place at higher additions (> 20wt% Ru).

As the E_p value varies with the nature of the electrode, the electrocatalytic activities of ternary composites towards oxidation of ethanol have been compared at a common and constant potential, E = 0.846 V *vs* RHE. At this potential, the oxidation current for EOR at each electrode on forward scan was noted and the results, so obtained, are displayed in Fig. (**5**). This figure clearly demonstrates that the performance of the composite electrode with 20wt% Ru is

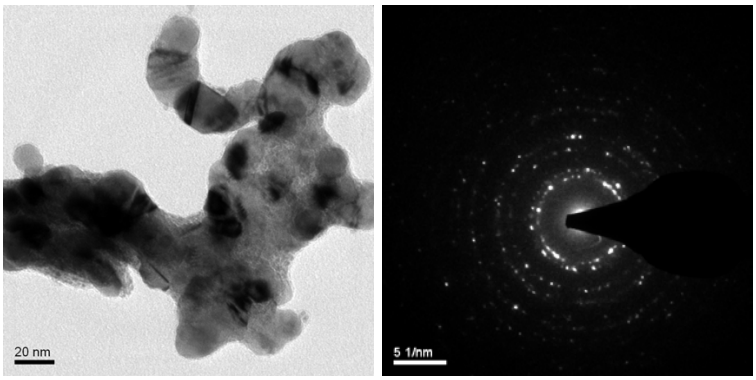

(a) (b)

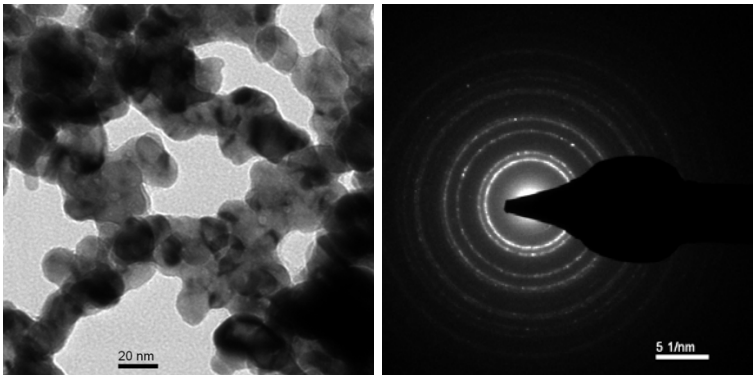

(c) (d)

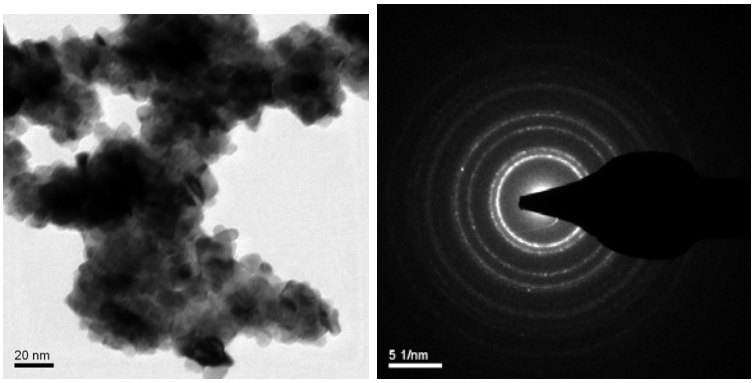

(e) (f)

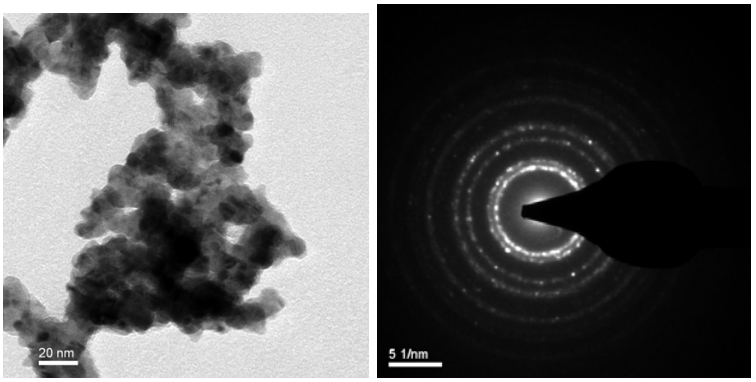

(g) (h)

Fig. (2). TEM pictures of pure Pd (**a**, **b**), Pd-0.5wt% C (**c**, **d**), Pd-0.5wt% C-5wt% Ru (**e**, **f**) and Pd-0.5wt% C-20wt% Ru (**g**, **h**) electrodes.

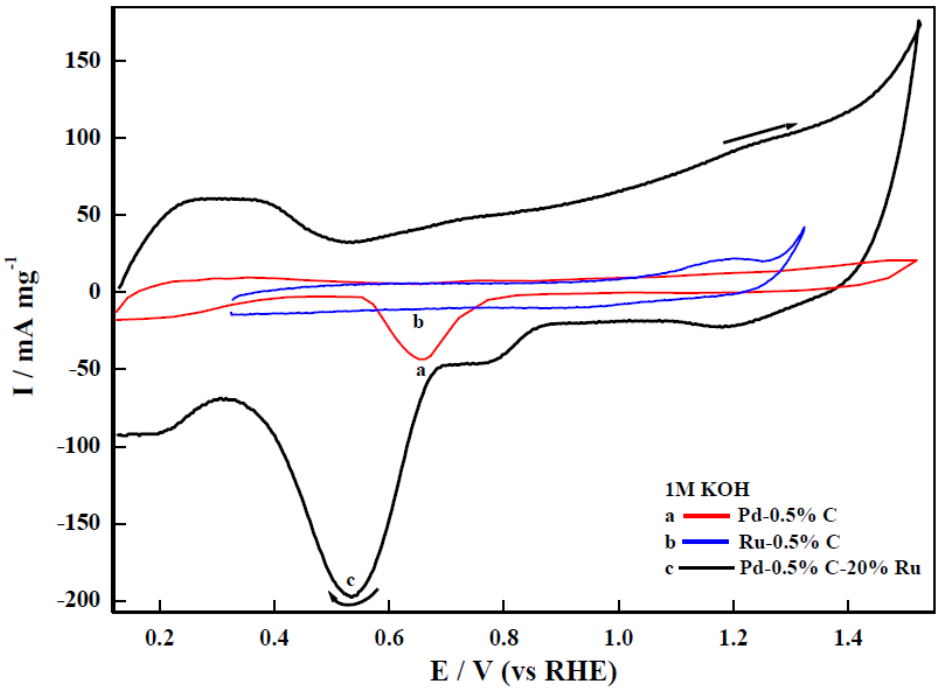

Fig. (3). Cyclic voltammograms of Pd-0.5wt% C, Ru-0.5wt% C and Pd-0.5wt% C-20wt% Ru composite in 1 M KOH at 298 K.

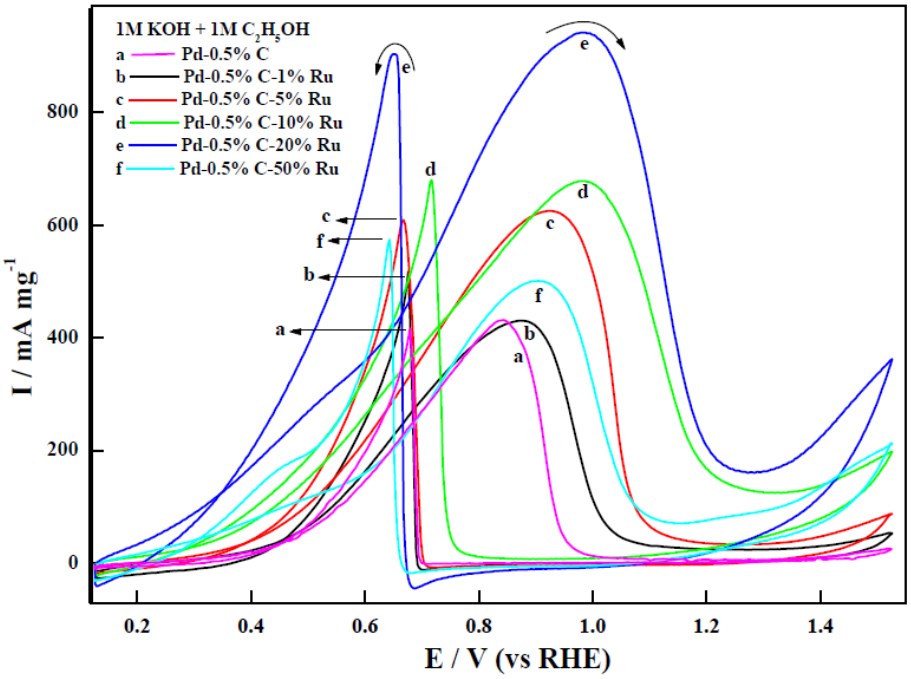

Fig. (4). Cyclic voltammograms for Pd-0.5wt% C and Pd-0.5wt% C-x wt% Ru electrodes in 1 M KOH + 1 M C_2H_5OH at 298 K.

the best one. This electrode has increased the rate of oxidation of ethanol by ~2 times as compared to that of oxidation of ethanol on the base (Pd-0.5wt% C) electrode. It is noteworthy that under similar experimental conditions, the electrocatalytic performance of the active electrode, Pd-0.5wt% C-20wt% Ru ($I_p \approx 1215$ mA mg_{Pd}^{-1}, $E_p \approx 0.976$ V *vs* RHE) of the present investigation is much higher than those of Pd-NiO (6:1)/C (ethanol: $I_p \approx 317$ mA mg_{Pd}^{-1}, $E_p \approx 0.846$ V *vs* RHE), Pd-Co_3O_4 (4:1)/C (ethanol: $I_p \approx 157$ mA mg_{Pd}^{-1}, $E_p \approx 0.786$ V *vs* RHE) and Pd-Mn_3O_4(4:1)/C (ethanol: $I_p \approx 190$ mA mg_{Pd}^{-1}, $E_p \approx 0.846$ V *vs* RHE) [41] electrodes recently reported in the literature. However, our electrode exhibited lower activity than the electrodes, Pd-MWCNT ($I_p \approx 2100$ mA mg_{Pd}^{-1}, $E_p \approx -0.12$ V *vs* Ag/AgCl/KCl_{sat}) [17] and Pd-Ni-Zn/C ($I_p \approx 3600$ mA mg_{Pd}^{-1}, $E_p \approx -0.15$ V *vs* Ag/AgCl/KCl_{sat}) [24]. Moreover, the electrocatalytic activities of the latter electrodes were tested in much higher concentrations of C_2H_5OH (10%) as well as KOH (2M).

Table 1. Results of Cyclic Voltammetry of Pd-0.5wt% C-x wt% Ru Composites on GC Electrodes in 1 M KOH + 1 M C_2H_5OH at 298 K

Amount of Ru (wt%)	Loading/ mg cm^{-2}	Area/cm^2	Onset potential/ mV *vs* RHE	Forward scan		Reverse scan	
				E_p/mV *vs* RHE	I_p/mA mg^{-1} Catalyst	E_p/mV *vs* RHE	I_p/mA mg^{-1} Catalyst
0	0.15	0.50	371	868	436.0	676	435
1	0.18	0.39	362 ± 8	860 ± 8	376 ± 9	686 ± 9	582± 33
2	0.18	0.43	338 ± 7	921 ± 3	496± 13	681 ± 2	499± 25
5	0.23	0.44	350 ± 13	916 ± 4	601± 20	669 ± 3	609 ± 9
10	0.23	0.43	320 ± 14	978 ± 3	670± 8	692 ± 3	667± 13
20	0.22	0.43	308 ± 19	975 ± 4	966± 24	650 ± 3	921± 19
30	0.23	0.41	332 ± 7	876 ± 18	500± 13	653 ± 2	545 ± 9
50	0.22	0.41	352 ± 4	892 ± 10	490 ± 2	639 ± 5	547± 17

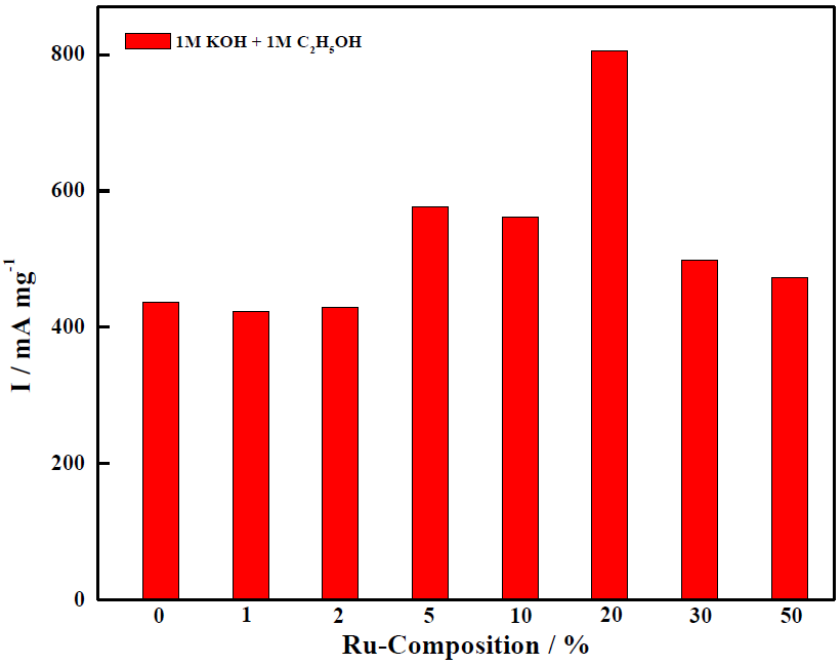

Fig. (5). Comparative electrocatalytic activities of different electrodes towards ethanol oxidation at E = 0.846 V *vs* RHE.

To examine the role of Ru in electrocatalysis of alcohol oxidation, CVs of Ru-0.5wt% C (without containing Pd) in 1 M KOH with and without containing 1 M C_2H_5OH were recorded under similar experimental conditions and the results are shown in Fig. (**6**). In blank solution, CV curve shows an anodic peak at E = 1.216 V *vs* RHE followed by the current peak for the oxygen evolution reaction. The observed anodic peak can be attributed to the oxidation of Ru to a higher valence state. The Pourbaix diagram for the Ru-H_2O system indicates the existence of Ru as $RuO_2.2H_2O$ (i.e. Ru (IV) state) at pH 14 (1M KOH). However, the cathodic peak corresponding to the observed anodic peak is not clearly indicated in the reverse scan.

The comparison of CVs of Ru-0.5wt% C, in presence and absence of alcohol, indicates that the oxidation of alcohol takes place at the Ru-0.5wt% C electrode with the E_{op} value of ~0.976 V *vs* RHE. But, the E_{op} values for alcohol oxidation at Pd-0.5wt% C-x wt% Ru composite electrodes are considerably low (0.496 – 0.266 V *vs* RHE) compared to one obtained on Ru-0.5wt% C. This result demonstrates that the oxidation of C_2H_5OH takes place mainly at the Pd sites in the composite.

The enhanced activities of composite electrodes can be ascribed to the greater affinity of Ru towards the water molecules forming the surface adsorbed OH molecule [42]. In fact, compared to Pd, Ru has the ability to activate water molecules at a lower potential. This facilitates the oxidation of adsorbed CO at lower potential [1]. Thus, the displacement of the E_{op} in a negative direction in the case of the catalysts containing Ru compared to Pd-0.5wt% C is mainly related to the bi-functional mechanism, where the beneficial effect is related to the formation of Ru-OH species at low potentials, which promotes the oxidation of adsorbed CO [35, 43].

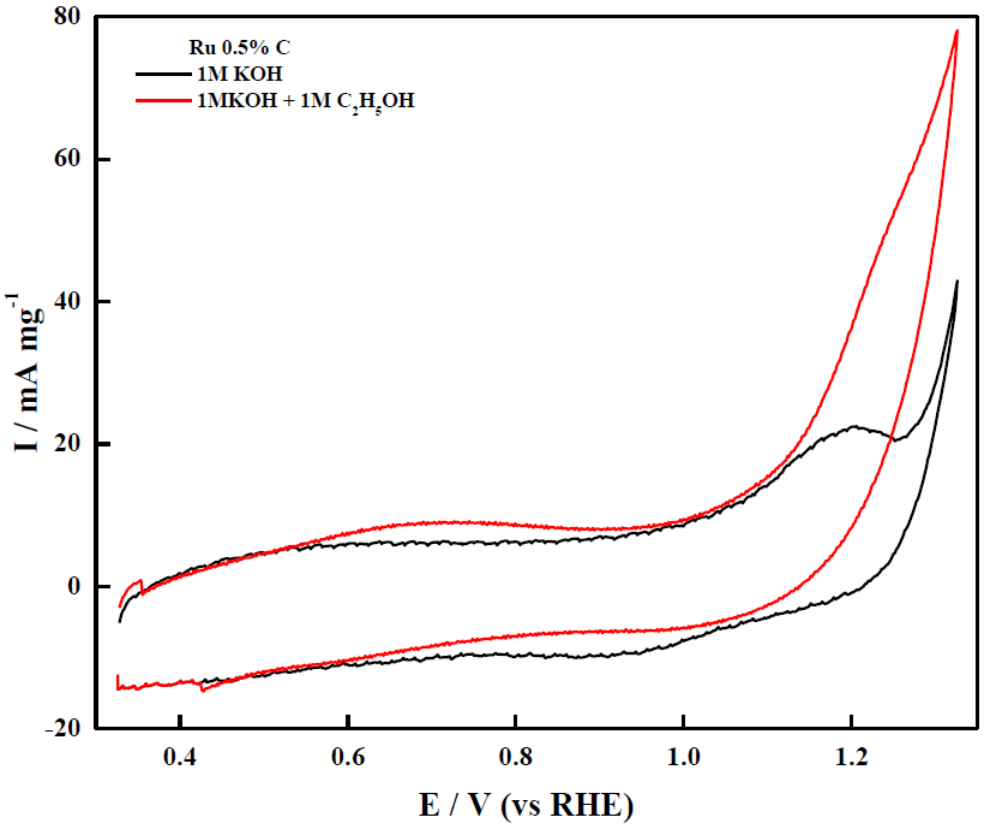

Fig. (6). Cyclic voltammograms for Ru-0.5wt% C in 1 M KOH with and without containing 1 M ethanol at 298 K.

3.3. Electrochemical Impedance Spectroscopy (EIS)

The impedance study of three ternary composite electrodes, namely Pd-0.5wt%C-5wt%Ru, Pd-0.5wt%C-10wt%Ru and Pd-0.5wt%C-20wt% Ru have been performed in the frequency range 0.01 - 10 x 10^3 Hz at a constant dc potential, 0.526 V *vs* RHE in 1 M KOH + 1 M C_2H_5OH and results are shown in Fig. (**7**). Also, the active electrode of this series was subjected to the EIS study at five different dc potentials, 0.326, 0.376, 0.426, 0.476 and 0.526 V *vs* RHE in 1 M KOH + 1 M C_2H_5OH and EIS spectra, so obtained, are displayed in Fig. (**8**). Before recording the EIS spectrum at a potential, the electrode was equilibrated at that potential for 300s.

All the EIS spectra shown in Figs. (**7**, **8**) look to be similar. They show a small arc at high (10 kHz – 3 kHz) and a semicircle at intermediate frequencies (3 kHz – 0.05 mHz). At low frequencies, the impedance curve tends to show the diffusional behavior. In fact, the capacitive component of the

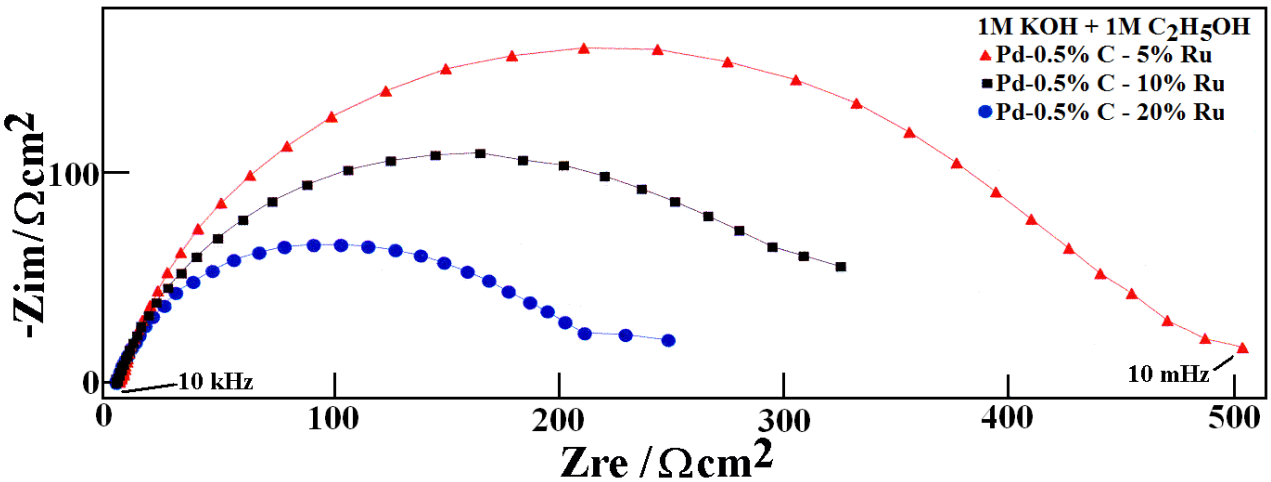

Fig. (7). The Nyquist plots of electrodes at E = 0.526 V *vs* RHE in 1 M KOH + 1 M C_2H_5OH at 298 K.

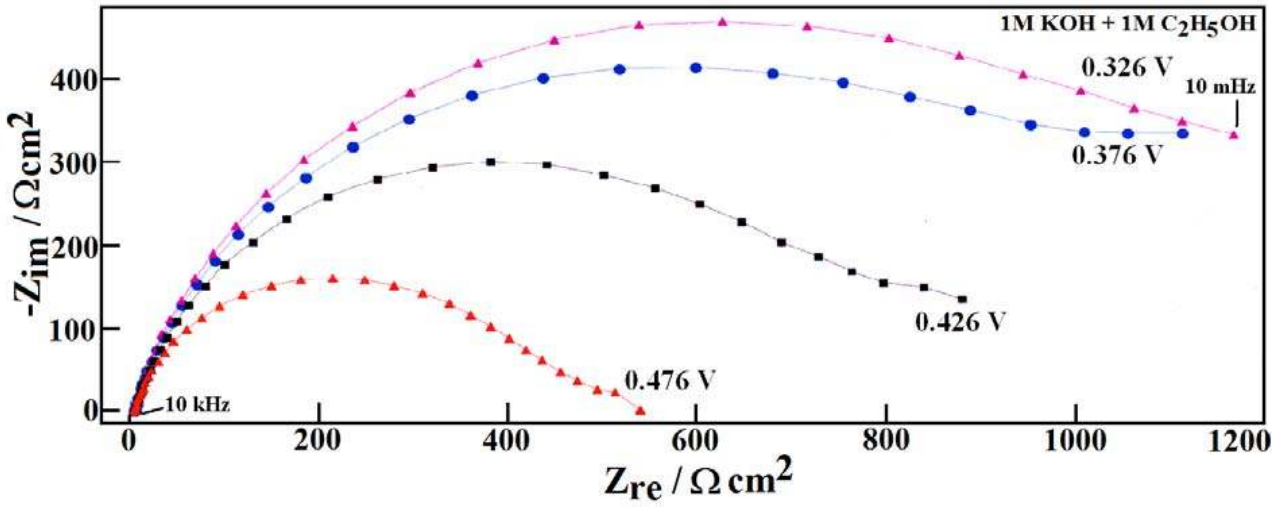

Fig. (8). Nyquist plots of Pd-0.5wt%C-20wt% Ru composite electrode at different dc potentials in 1 M KOH + 1 M C_2H_5OH at 298 K.

impedance gradually decreases with decrease in frequency, particularly at very low frequencies.

Fig. (**7**) shows that the diameter of the semi circle decreases with the increase in Ru content in the composite. Further, the increase in dc potential seems to affect the diameter of the semicircle greatly, but high frequency arc is only little influenced. It is observed that as the potential increases, the diameter of semicircle decreases. Thus, results show that the decrease in diameter of the semicircle with the increase in potential is mainly caused due to the increase in the rate of EOR. The nature of impedance curve at very low frequencies can be attributed to manifestation of complex processes such as mass transfer, adsorption of reaction intermediates/products, etc. In view of interference of the latter in analysis, the experimental EIS data obtained between 10 kHz and 0.5 Hz have been simulated.

The electrical equivalent circuit model, R_s (Q_f (R_f (C_{dl} R_{ct}))), was employed to simulate the experimental data of the present electrode-electrolyte system. Symbols: R_s, R_f, R_{ct}, Q_f and C_{dl} represent the solution resistance, catalyst-film resistance, charge transfer resistance, constant phase element (CPE) and double layer capacitance, respectively. It is observed that the simulated impedance data based on proposed circuit model agreed excellently with those experimentally observed ones in the frequency range (10 kHz to 0.5 Hz). In case of the electrode, Pd-5wt%C-20wt%Ru, the simulated and experimental curves in Nyquist and Bode representations are shown in Fig. (**9**) and the estimates of the equivalent circuit parameters are given in Table **2**.

Table **2** shows that introduction of Ru decreases the R_{ct} greatly and hence increases the rate for OER. Thus, the Pd-5wt%C-20wt%Ru electrode is the greatest active among the series. Exactly, the same conclusion has also been derived from the CV study.

3.4. Chronoamperometry

Chronoamperograms of base and active electrodes, namely Pd-0.5wt% C, Pd-0.5wt% C-5wt% Ru, Pd-0.5wt% C-10wt% Ru, and Pd-0.5wt% C-20wt% Ru recorded at E = 0.726 V *vs* RHE in 1 M KOH + 1 M C_2H_5OH and shown in Fig. (**10**) demonstrate that the performance as well as poisoning tolerance of the composite, Pd-0.5wt% C-20wt% Ru, towards ethanol oxidation is the highest among the electrodes investigated. This is also quite evident from values of the ethanol oxidation currents noted from Fig. (**10**) at the end of 120 min; values were 5.9, 63.6, 78.5, and 89.0 mA mg^{-1} on Pd-0.5wt% C, Pd-0.5wt% C-5wt% Ru, Pd-0.5wt% C-10wt% Ru, and Pd-0.5wt% C-20wt% Ru, respectively.

3.5. Reaction Products Analyses

Chronoamperometry of the active Pd-0.5wt% C-20wt% Ru was carried out in an H-cell containing 1 M KOH + 1 M C_2H_5OH at E = 0.726 V *vs* RHE for 5 h. After the experiment was over, the cell solution of anodic compartment was withdrawn and to this added $BaCl_2$ solution to precipitate CO_3^{2-}, if any, as $BaCO_3$. The solid residue, so obtained, was filtered, repeatedly washed with distilled water, and tested for the presence of CO_3^{2-}. Mixed the filtrate and washings, neutralized with dilute HCl and added $FeCl_3$ solution to test the presence of CH_3COO^-. Results indicated the presence of both CO_3^{2-} and CH_3COO^-. Further, the cyclic voltammogram for the Pd-0.5wt% C-20wt% Ru electrode in 1 M KOH + 1 M CH_3COOK did not indicate any oxidation of potassium acetate. Thus, results of this test corroborate the findings of previous studies reported in [44].

CONCLUSION

The study reveals that the Ru addition greatly improves the electrocatalytic activity of the Pd-0.5wt% C electrode; the improvement, however, being the greatest with composite electrode containing 20wt% Ru. The latter electrode has demonstrated 2-3 times higher electrocatalytic activity compared to the base electrode (Pd-0.5wt%C). The poisoning tolerance of this electrode towards oxidation intermediates was also the greatest.

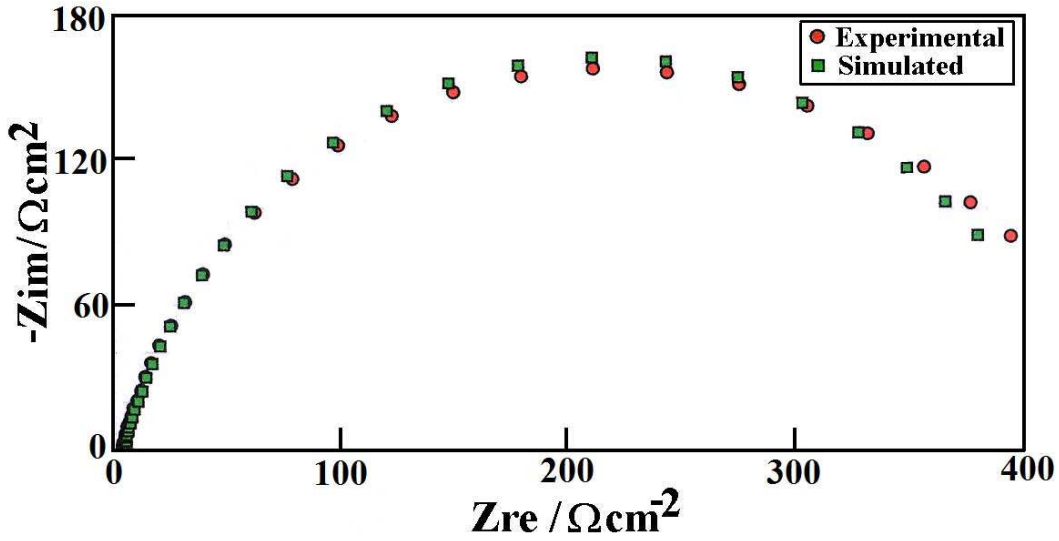

(a)

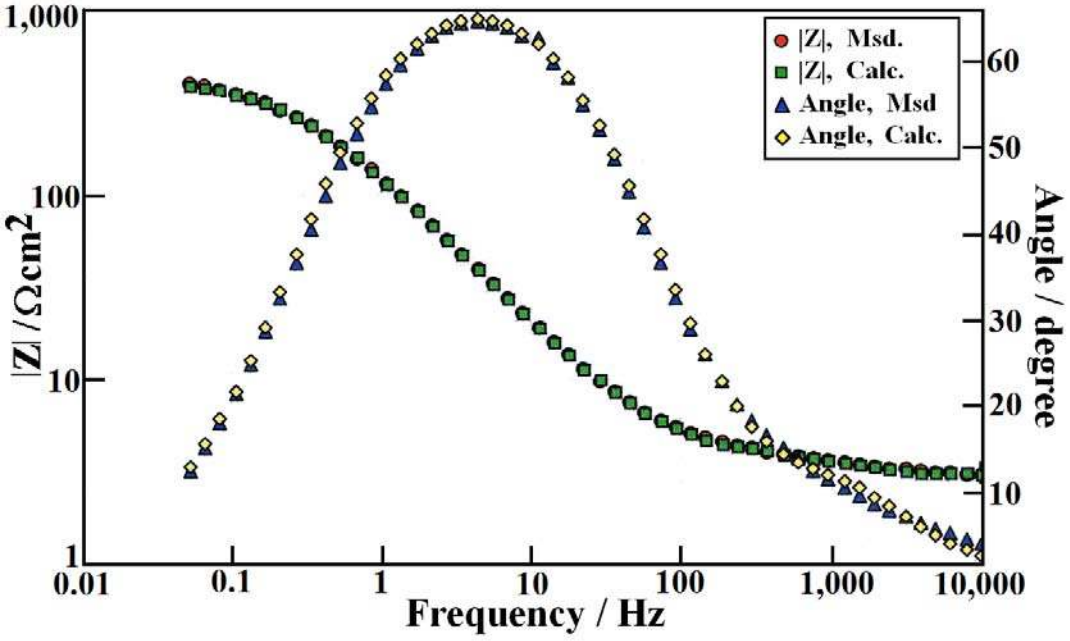

(b)

Fig. (9). Experimental and simulated Nyquist (**a**) and Bode (**b**) plots of Pd-0.5wt%C-20wt% Ru electrode in 1 M KOH + 1 M C_2H_5OH at 0.526 V *vs* RHE.

Table 2. Estimates of Equivalent Circuit Parameters for Composite Electrodes in 1 M KOH + 1 M C_2H_5OH at E = 0.526 V *vs* RHE

Amount of Ru/wt%	Rs/Ω cm^2	10^3Q/F s^{n-1} cm^{-2}	n	R_f/Ω cm^2	10^4C_{dl}/F cm^{-2}	R_{ct}/Ω cm^2
0	1.33	1.76	0.70	2.30	3.30	55.2
5	3.06	1.50	0.84	424.3	3.73	0.72
10	3.08	1.60	0.85	422.0	4.54	0.78
20	1.39	3.82	0.81	187.4	8.82	0.59

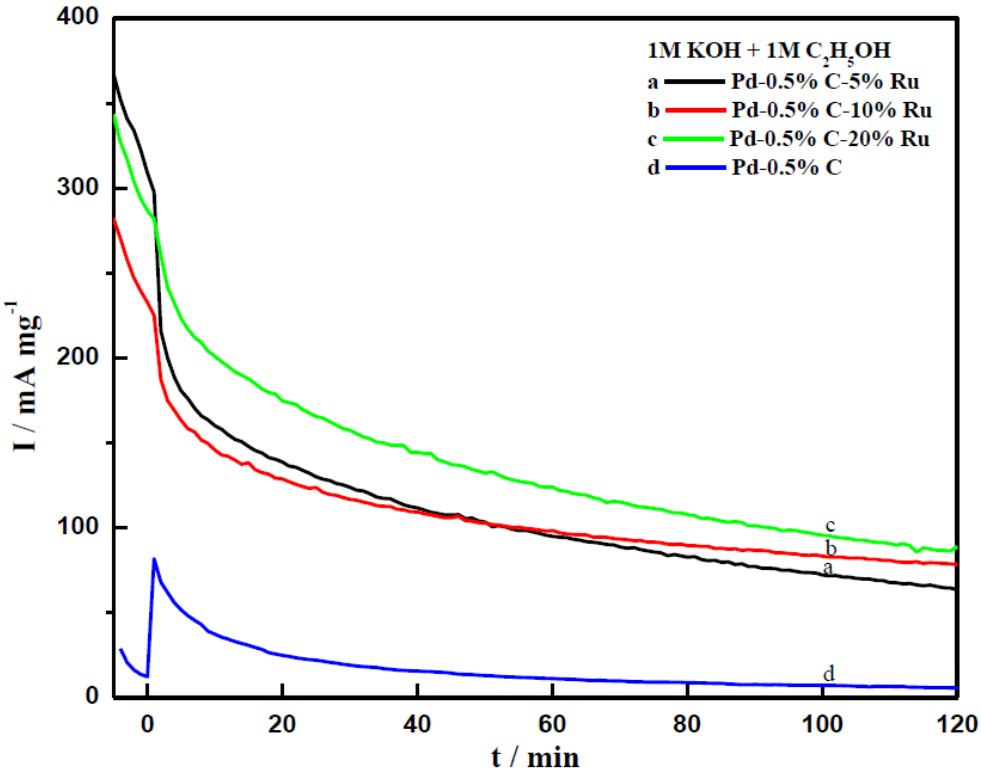

Fig. (10). Chronoamperograms for Pd-0.5wt% C and Pd-0.5wt% C-x wt% Ru electrodes in 1 M KOH + 1 M C_2H_5OH at 298 K.

ACKNOWLEDGEMENTS

The financial supports received from the Department of Science and Technology, DST (Project SR/S1/PC-41) and Council of Scientific and Industrial Research, CSIR (Sch. No. 01(2320/09/EMR-II), Government of India New Delhi are gratefully acknowledged. One of authors (Anindita) thanks the Council of Scientific and Industrial Research (CSIR) New Delhi for the award of Senior Research Fellowship. We thank Prof. Gouthama, Department of Material and Metallurgical Engineering, I.I.T. Kanpur for TEM analyses.

REFERENCES

[1] Selvaraj, V.; Vinoba, M.; Alagar, M.J. Electrocatalytic oxidation of ethylene glycol on Pt and Pt-Ru nanoparticles modified multi-walled carbon nanotubes. *J. Colloid Interface Sci.*, **2008**, *322*, 537-544.

[2] Lamy, C.; Lima, A.; Rhun, V.L.; Delime, F.; Coutanceau C.; Léger, J.-M. Recent advances in the development of direct alcohol fuel cells. *J. Power Sources*, **2002**, *105*, 283-296.

[3] Antolini, E. Catalysts for direct ethanol fuel cells. *J. Power Sources*, **2007**, *170*(1) 1-12.

[4] Bianchini, C.; Shen, P.K. Palladium based electrocatalysts for alcohol oxidation in half cells and in direct alcohol fuel cells. *Chem. Rev.*, **2009**, *109*, 4183-4206.

[5] Gupta S.S.; Datta, J. Electrode kinetics of ethanol oxidation on novel CuNi alloy supported catalysts synthesized from PTFE suspension. *J. Power Sources*, **2005**, *145*, 124-132.

[6] Lamy, C.; Rousseau, S.; Belgsir, E. M.; Coutanceau, C.; Léger, J.-M. Recent progress in the direct ethanol fuel cell: development of new platinum-tin electrocatlysts. *Electrochim. Acta*, **2004**, *49*, 3901-3908.

[7] Antolini, E. Carbon Support for low-temperature fuel cell catalysts. *Appl. Catal. B.*, **2009**, *88*, 1-24.

[8] Gupta, S.S.; Singh, S.; Datta, J. Temperature effect on the electrode kinetics of ethanol electro-oxidation on Sn modified Pt catalyst through voltammetry and impedance spectroscopy. *Mater. Chem. Phys.*, **2010**, *120*, 682-690.

[9] Singh, R.N.; Awasthi, R.; Tiwari, S.K. Electrocatalytic activity of binary nanocomposites of Pt and nanocarbon/multiwall carbon nanotube for methanol electrooxidation. *TOCJ,* **2010**, *3*, 54-61.

[10] Platinum 2008 Interim Review. *Platinum Metals Rev.*, **2009**, *53*, 48-49.

[11] Lee, C.-L. Synthesis and electrocatalytic activity of carbon-nanomaterials-supported Pd nanoparticles from self-regulated reduction of sodium n-dodecyl sulfate. *J. Solid State Electrochem.*, **2007**, *11*, 1313-1317.

[12] Lee, C.-L.; Huang, Y.-C.; Kuo L.C.; Lin, Y.-W. Preparation of carbon nanotubes supported Pd nano particle by self-regulated reduction of surfactants. *Carbon*, **2007**, *45*, 203-206.

[13] Wang, M.; Guo D.-J.; Li, H.-L. High activity of novel Pd/TiO_2 nanotube catalysts for methanol electrooxidation. *J. Solid State Chem.*, **2005**, *178*, 1996-2000.

[14] Zhang, F.-B.; Li, H.-L. One step synthesis of Pd/C composite *via* a microwave assisted ionic liquid method and its electrocatalytic characteristics. *Carbon*, **2006**, *44*, 3195-3198.

[15] Zhang, K.-F.; Guo, D.-J.; Liu, X.; Li, J.; Li, H.-L.; Su, Z.-X. Vanadium oxide nanotubes as the support of Pd catalysts for methanol oxidation in alkaline solution. *J. Power Sources*, **2006**, *162*, 1077-1081.

[16] Shen, P.K.; Xu, C. Alcohol oxidation on nanocrystalline oxide Pd/C promoted electrocatalysts. *Electrochem. Commun.*, **2006**, *8*, 184-188.

[17] Bambagioni, V.; Bianchini, C.; Marchionni, A.; Filippi, Z.; Vizza, F.; Teddy, J.; Serp P.; Zhiani, M. Pd and Pt-Ru anode eletrocatalysts supported on multiwalled carbon tubes and their use in passive and active direct alcohol fuel cells with an anion-exchange membrane (alcohol: methanol, ethanol, glycerol). *J. Power Sources*, **2009**, *190*, 241-251.

[18] Spendelow, J.S.; Wieckowski, A. Electrocatalysis of oxygen reduction and small alcohol oxidation in alkaline media. *Phys. Chem. Chem. Phys.*, **2007**, *9*, 2654-2675.

[19] Vigier, F.; Rousseau, S.; Coutanceau, C.; Léger, J.-M.; Lamy, C. Electrocatalysis for the direct alcohol fuel cell. *Top. Catal.*, **2006**, *40*, 111-121.

[20] Shen, P.K.; Xu, C.; Zeng, R.; Liu, Y. Electro-oxidation of methanol on NiO-promoted Pt/C and Pd/C Catalysts. *Electrochem. Solid State Lett.*, **2006**, *9*, A39-A42.

[21] Hu, F.P.; Cui, G.F.; Wei, Z.D.; Shen, P.K. Improved kinetics of ethanol oxidation on Pd catalysts supported on tungsten carbide/carbon nanotubes. *Electrochem. Commun.*, **2008**, *10*, 1303-1306.

[22] Hu, F.; Chen, C.; Wang, Z.; Wei, G.; Shen, P.K. Mechanistic study of ethanol oxidation on Pd-NiO/C electrocatalyst. *Electrochim. Acta*, **2006**, *52*, 1087-1091.

[23] Chu, D.; Wang, J.; Wang, S.; Zha, L.; He, J.; Hou, Y.; Yan, Y.; Lin H.; Tian, Z. High activity of Pd-In_2O_3/CNT electrocatalysts for electro-oxidation of ethanol. *Catal. Commun.*, **2008**, *10*, 955-958.

[24] Bianchini, C.; Bambagioni, V.; Filippi, J.; Marchionni, A.; Vizza, F.; Bert, P.; Tampucci, A. Selective oxidation of ethanol to acetic acid in highly efficient polymer electrolyte membrane-direct ethanol fuel cells. *Electrochem. Commun.*, **2009**, *11*, 1077-1080.

[25] Bagchi, J.; Bhattacharya, S.K. Electrocatlytic activity of binary palladium ruthenium anode catalyst on Ni-support for ethanol alkaline fuel cells. *Trans. Metal Chem.*, **2007**, *32*, 47-55.

[26] Fang, X.; Wang, L.; Shen, P.K.; Cui, G.; Bianchini, C. An in situ fourier transform infrared spectroelectrochemical study on ethanol electrooxidation on Pd in alkaline solution. *J. Power Sources*, **2010**, *195*, 1375-1378.

[27] Singh, R.N.; Singh, A.; Anindita. Electrocatalytic activity of binary and ternary composite films of Pd, MWCNT, and Ni for ethanol electrooxidation in alkaline solutions. *Carbon*, **2009**, *47*, 271-278.

[28] Singh, R.N.; Anindita: Singh, A.; Mishra, D. Composite films of Pd, nanocarbon and Ni for ethanol electrooxidation. *Proc. ICNM,* **2009**, *I*, 255-267.

[29] Singh, R.N.; Singh, A.; Anindita. Electrocatalytic activity of binary and ternary composite films of Pd, MWCNT, and Ni, Part II; Methanol electrooxidation in 1M KOH. *Int. J. Hydrogen Energy*, **2009**, *34*, 2052-2057.

[30] Singh, R.N.; Singh, A.; Anindita. Electrocatalytic activities of binary and ternary composite electrodes of Pd, nanocarbon and Ni for electrooxidation of methanol in alkaline medium. *J. Solid State Electrochem.*, **2009**, *13*, 1259-1265.

[31] Awasthi, R.; Anindita; Singh, R.N. Synthesis and characterization of nanostructured Pd-Ni and Pd-Ni-C composites towards electrooxidation of alcohols. *TOCJ*, **2010**, *3*, 70-78.

[32] Petrii, Oleg A. Pt-Ru electrocatalysts for fuel cells: A representative review. *J. Solid State Electrochem.*, **2008**, *12*, 609-642.

[33] Huang, J.; Liu, Z.; He, C.; Gan, L.M. Synthesis of PtRu nanoparticles from the hydrosilylation reaction and application as catalyst for direct methanol fuel cell. *J. Phys. Chem. B*, **2005**, *109*, 16644-16649.

[34] Raman, R.K.; Shukla, A.K.; Gayen, A.; Hegde, M.S.; Priolkar, K.R.; Sarode, P.R.; Emura, S. Tailoring a Pt-Ru catalysts for enhanced methanol electro-oxidation. *J. Power Sources*, **2006**, *157*, 45-55.

[35] Wang, J.; Xi, J.; Bai, Y.; Shen, Y.; Sun, J.; Chen, L.; Zhu W.; Qiu, X. Structural designing of Pt-CeO_2/CNTs for methanol electrooxidation. *J. Power Sources*, **2007**, *164*, 555-560.

[36] Singh, R.N.; Mishra, D.; Anindita; Sinha, A.S.K.; Singh, A. Novel electrocatalysts for generating oxygen from alkaline water electrolysis. *Electrochem. Commun.*, **2007**, *9*, 1369-1373.

[37] Singh, R.N.; Koenig, J.-F.; Poillerat, G.; Chartier, P. Electrochemical studies on protective thin Co_3O_4 and $NiCo_2O_4$ films prepared on Ti by spray pyrolysis for oxygen evolution. *J. Electrochem. Soc.*, **1990**, *137*, 1408-1413.

[38] Shobha, T.; Arvinda, C.L.; Bera, P.; Devi, G.; Mayanna, S.M. Characterization of Ni-Pd alloy as anode for methanol oxidative fuel cell. *Mater. Chem. Phys.,* **2003**, *80*, 656-661.

[39] Liu, J.; Ye, J.; Xu, C.; Jiang, S.P.; Tong, Y. Kinetics of ethanol electrooxidation at Pd electrodeposited on Ti. *Electrochem. Commun.*, **2007**, *9*, 2334-2339.

[40] Huang, W.; Li, Z.L.; Peng, Y.D.; Chen, S.; Zheng J.F.; Niu, Z.J. Oscillatory electrocatalytic oxidation of methanol on an $Ni(OH)_2$ film electrode. *J. Solid State Electrochem.*, **2005**, *9*, 284-289.

[41] Xu, C.; Tian, Z.; Shen, P.K.; Jiang, S.P. Oxide (CeO_2, NiO, Co_3O_4 and Mn_3O_4)-promoted Pd/C electrocatalysts for alcohol electrooxidation in alkaline media. *Electrochim. Acta*, **2008**, *53*, 2610-2618.

[42] Casella, I.G. Electrooxidation of aliphatic alcohols on palladium oxide catalyst prepared by pulsed electrodeposition technique. *Electrochim. Acta*, **2009**, *54*, 3866-3871.

[43] Liang, Z.X.; Zhao, T.S.; Xu, J.B.; Zhu, L.D. Mechanism study of the ethanol oxidation reaction on Pd in alkaline media. *Electrochim. Acta*, **2009**, *54*, 2203-2208.

Received: September 30, 2010 Revised: November 11, 2010 Accepted: December 7, 2010